


## Article

# Projecting Future Land Use Evolution and Its Effect on Spatiotemporal Patterns of Habitat Quality in China

Yiqing Chen <sup>1,2</sup>, Fengyu Zhang <sup>1</sup> and Jinyao Lin <sup>1,2,\*</sup> 

<sup>1</sup> School of Geography and Remote Sensing, Guangzhou University, Guangzhou 510006, China; 1901500034@e.gzhu.edu.cn (Y.C.); 32201400030@e.gzhu.edu.cn (F.Z.)

<sup>2</sup> Huangpu Research School of Guangzhou University, Guangzhou 510006, China

\* Correspondence: ljy2012@gzhu.edu.cn

**Abstract:** In recent years, irrational land development has caused significant habitat quality problems. Previous habitat quality studies have mainly concentrated on medium- and small-sized areas, and few studies have conducted a comprehensive long-term analysis of terrestrial habitat quality in large countries. Accordingly, this research aimed to identify the changes in land use and habitat quality in China during the last four decades. The InVEST method was employed for evaluating China's habitat quality. This evaluation included both habitat degradation and habitat quality scores. Then, the FLUS and InVEST methods were combined to project future land use evolution in China through 2050 and assess its effect on habitat quality. Our study demonstrated a robust connection between habitat quality and the spatial distribution of land use classes, topography, and resource availability. Furthermore, over the past four decades, high-quality habitats in the country have been degrading and shrinking, while low-quality habitats have been expanding. The projection results indicate that the habitat problems in China will become increasingly severe over the coming decades. Our study suggests that the habitat quality in China should be improved by optimizing land use patterns, stabilizing areas with optimal habitat conditions, and restoring degraded habitats.

**Keywords:** habitat quality; wildlife habitat; land use and cover change; conservation; urban sprawl; China



Academic Editor: Nathan J. Moore

Received: 17 December 2024

Revised: 17 January 2025

Accepted: 20 January 2025

Published: 21 January 2025

**Citation:** Chen, Y.; Zhang, F.; Lin, J. Projecting Future Land Use Evolution and Its Effect on Spatiotemporal Patterns of Habitat Quality in China. *Appl. Sci.* **2025**, *15*, 1042. <https://doi.org/10.3390/app15031042>

**Copyright:** © 2025 by the authors. Licensee MDPI, Basel, Switzerland. This article is an open access article distributed under the terms and conditions of the Creative Commons Attribution (CC BY) license (<https://creativecommons.org/licenses/by/4.0/>).

## 1. Introduction

Irrational land use development is a major cause of land degradation [1–3]. This phenomenon involves a range of inappropriate land use practices, including inefficient land resource allocation, unbalanced land use, and unsustainable land management strategies. In particular, China's urbanization has been gradually speeding up since the reform and opening up [4–6]. A considerable proportion of the country's ecological resources, including forests, cropland, and grassland, have been encroached upon by construction land [7–10]. Habitat quality is defined as the capacity of an ecosystem to offer desirable living environments for species [11–13]. Habitat quality is a critical indicator of the functionality and integrity of ecosystem services. Nevertheless, the intensification of land use development has resulted in a notable degradation of habitat quality [14–17].

Related studies have focused on two main parts: habitat quality for a single species and overall habitat quality. While species-specific assessments provide detailed insights, they are often limited in scope and scalability [18–20]. Consequently, an increasing number of studies are using mathematical methods, including habitat suitability, the SolVES model, and the InVEST model, to assess regional habitat quality. Among them, InVEST is the most

extensively used and has reached a high level of maturity [21–23]. This model includes a wide range of tools, including habitat quality, carbon storage, and soil conservation. The habitat quality tool is capable of deriving grid-scale habitat quality results according to land use and threat factors. The methodology has been applied by numerous studies in a variety of regions [24–26]. Nevertheless, the InVEST method is insufficient to project future habitat quality conditions. It needs to be further coupled with land use simulation models.

Among the various land use simulation approaches, cellular automata (CA) are the most prevalent [27–31]. The CA approach effectively simulates complex land use evolution by applying simple transition rules [32–35]. Notably, Liu et al. [36] proposed an advanced FLUS model, which builds upon the traditional CA, to account for the complex interaction among various land use classes and to improve the accuracy of land use projection. Currently, the FLUS method has been extensively utilized to simulate land use evolution [37–39]. Consequently, the FLUS and InVEST models can be integrated to project future changes in habitat quality.

In particular, given the scarcity of available land resources and the equally important need to protect and develop them, it is of particular significance to combine habitat quality assessment and land use projection [40–42]. Recent studies have demonstrated that the integration of InVEST and FLUS models has significant value for predicting future changes in habitat quality. However, the majority of relevant studies have been limited to medium- and small-sized regions, including watersheds, provinces, municipalities, and ecological zones. Few studies have analyzed the spatial and temporal evolution of habitat quality at a large national scale over a long period of time.

At the regional scale, Gomes et al. [43] employed these two models to assess the dynamic changes in habitat quality under different scenarios in Lithuania, highlighting the influence of land use on habitat quality. Raji et al. [44] used these two models to simulate habitat quality trends under four land use scenarios in the Sokoto-Rima Basin, Nigeria, and found that sustainable development scenarios could significantly improve biodiversity. Fida et al. [45] projected the impact of land use evolution on habitat quality in southwestern Ethiopia by combining InVEST and FLUS models. Rahimi et al. [46] projected future habitat quality and its response to land use evolution in southwestern Iran based on InVEST and CA models. Overall, these regional studies indicate that while the integration of InVEST and FLUS models provides effective tools for predicting habitat quality, further refinement and validation are needed for long-term and large-scale applications.

In this regard, this research endeavors to fill the knowledge gaps in the literature from two perspectives. First, we aim to provide a long-term and nationwide assessment of the evolution of habitat quality in China over the past four decades. Second, we aim to project future land use evolution and its effect on the spatiotemporal patterns of habitat quality in China. This nationwide analysis will provide insights into both historical trends and future scenarios, supporting evidence-based conservation planning and policy development.

To this end, we employed the InVEST method to analyze the effect of China's land use evolution on habitat quality during 1980–2020. The FLUS–InVEST model was then utilized to project China's future land use evolution and its effect on habitat quality in 2050. Additionally, the causes of habitat quality changes were investigated, and corresponding recommendations were proposed. The objective of our study is to establish a foundation for decision makers to formulate sound land use and ecological design.

## 2. Data and Methods

### 2.1. Data

The national land use datasets were sourced from the Chinese Academy of Sciences [47]. This institution produced high-quality land use datasets from 1980 to 2020, with a resolution

of 1 km. Six land use classes have been identified from the datasets, including cropland, forests, grassland, water, construction land, and unused land. The remaining datasets required for the land use projection are the spatial driving factors, including climate and socioeconomic data from the Chinese Academy of Sciences, the elevation dataset from the Geographic and Spatial Data Cloud, and transportation and water system data from OpenStreetMap (Table 1). Furthermore, the technical framework of our research comprises two aspects: habitat quality assessment and land use projection (Figure 1).

**Table 1.** Attributes and sources of the datasets.

Category	Factor	Cell Size	Source
Climate	Mean annual temperature	1 km	Chinese Academy of Sciences
	Mean annual precipitation		
Socioeconomic	GDP	250 m	Geographic and Spatial Data Cloud
	Population		
Topography	Elevation	Vector	OpenStreetMap
	Slope		
	Aspect		
Traffic	Expressway	1 km	Chinese Academy of Sciences
	Railway		
	Road		
Limitation factor	Rivers and reservoirs		
Threat factor	Cropland	1 km	Chinese Academy of Sciences
	Urban land		
	Rural land		
	Other construction		

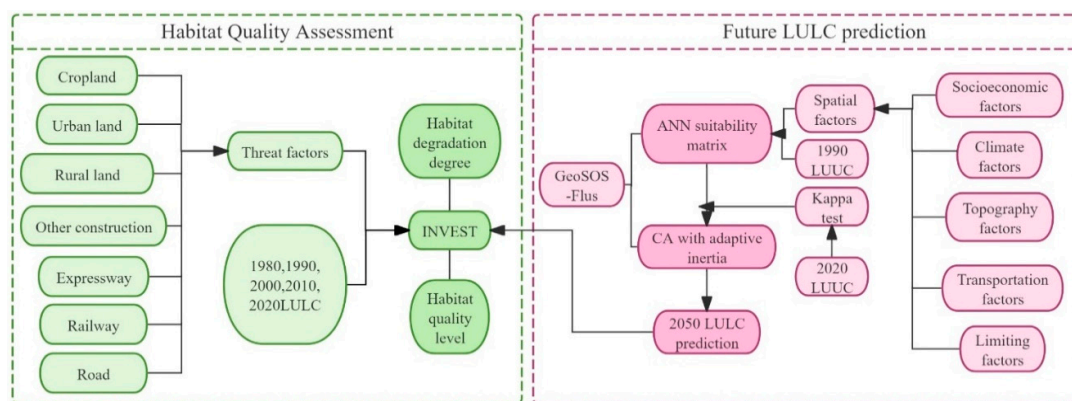


**Figure 1.** Technical framework of our research.

OpenStreetMap was selected due to three main advantages over China’s official transportation data: First, its crowdsourced nature ensures a higher frequency of transportation information updates. Second, it offers comprehensive coverage of geographical features with detailed transportation networks. Third, its open-access nature allows unrestricted use of the data for research purposes.

2.2. Methods

2.2.1. Investigation of Land Use

The evolution of different land use classes was analyzed from both spatial and temporal perspectives using transformation matrices. Subsequently, two land use indicators, the trend state index and the mean annual net change rate, were employed to assess the dynamic conditions of land use evolution. The trend state index can reveal the increas-

ing and decreasing states of land use over time. The calculation for this index ( $P_S$ ) is as follows [48,49]:

$$P_S = \frac{\Delta W_{in} - \Delta W_{out}}{\Delta W_{in} + \Delta W_{out}}, (\Delta W_{in} + \Delta W_{out} \neq 0) \tag{1}$$

where  $\Delta W_{in}$  is the total area of other land use classes transformed to the targeted land use class, and  $\Delta W_{out}$  is the total area of the targeted land use class transformed to other land use classes.

Furthermore, the annual net change rate ( $S_r$ ) reveals the speed of variation for a targeted land use class over time. This ( $S_r$ ) is calculated as follows [50,51]:

$$S_r = \left( \frac{1}{T} \cdot \frac{\Delta W_{in} - \Delta W_{out}}{W_i} \right) \times 100\% \tag{2}$$

where  $T$  means the time span, and  $W_i$  means the initial area of land use class  $i$ .

### 2.2.2. Investigation of Habitat Quality

The habitat quality tool of the InVEST method was adopted. This tool can effectively estimate the magnitude of habitat degradation at a fine scale, thereby enabling the calculation of habitat quality levels [52,53]:

$$Q_{xj} = H_j \times \left[ 1 - \left( \frac{D_{xj}^2}{D_{xj}^2 + k^2} \right) \right] \tag{3}$$

where  $Q_{xj}$  is the habitat quality in grid  $x$  within land use class  $j$ ,  $H_j$  is the habitat resilience for land use class  $j$ ,  $k$  is a fixed parameter typically set to 0.5, and  $D_{xj}$  is the habitat degradation level in grid  $x$  within land use class  $j$ :

$$D_{xj} = \sum_{r=1}^R \sum_{y=1}^{Y_r} \left( \frac{W_r}{\sum_{r=1}^R W_r} \right) r_y i_{rxy} \beta_x S_{jr} \tag{4}$$

where  $R$  is the number of threat factors,  $y$  represents a grid in threat factor  $r$ ,  $Y_r$  is the number of grids in that factor,  $W_r$  is the weight for threat factor  $r$ ,  $r_y$  is the value of factor  $r$  in grid  $y$ ,  $i_{rxy}$  is the threat degree of  $r_y$  to grid  $x$ ,  $\beta_x$  is the accessibility to grid  $x$ , and  $S_{jr}$  is the susceptibility of land use  $j$  to threat factor  $r$ , where  $i_{rxy}$  is assessed using the linear or exponential decay formula:

$$i_{rxy} = 1 - (d_{xy} / d_{r \max}) \text{ (linear)} \tag{5}$$

$$i_{rxy} = \exp[-(2.99 / d_{r \max}) \cdot d_{xy}] \text{ (exponential)} \tag{6}$$

where  $d_{xy}$  means the straight-line distance from grid  $x$  to grid  $y$ ,  $d_{r \max}$  means the maximum threat range for factor  $r$ .

The extensive use of chemical fertilizers and pesticides on cropland has become a significant threat to surrounding habitat quality in China. In addition, construction land and traffic networks have profound detrimental impacts on the environment. Therefore, considering both prior studies and the distinctive context in China, this research identified seven threat factors: cropland, three classes of construction land, and traffic networks.

The parameter settings for the threat factors in this study were primarily based on existing research findings. Urban land has the most significant impact on habitat, with multiple studies setting its weight between 0.8 and 1.0 [54–57]. Cropland was given a weight of 0.6, which aligns with the range of 0.5–0.68 established in existing studies [56], and rural land was also given a weight of 0.6, which is consistent with the findings in the

literature [58,59]. The weights for expressways and railways were set at 0.7 based on the findings of previous studies [56], while roads were assigned a lower weight of 0.5 [58,60].

In terms of spatial decay characteristics, an exponential decay function was adopted on the basis that the influence of point-source threats, such as urban land and rural land, decreases rapidly with distance. In comparison, a linear decay function was selected for linear features, such as cropland and transportation infrastructure [54,55,59]. The maximum influence distances for various factors were taken from related studies [55,56,60]: 10 km for urban land, 5–6 km for rural land, 1–3 km for cropland, and 3–8 km for transportation facilities. All these parameter settings are within reasonable ranges established by previous research. The maximum threat range, weight, and distance decay function were assigned to each threat factor based on previous studies (Table 2) [11,13,21,26,61,62].

**Table 2.** Features of threat factors.

Factor	Maximum Threat Range (Kilometer)	Weight	Distance Decay
Cropland	1	0.6	Linear
Urban land	10	1	Exponential
Rural land	5	0.6	Exponential
Other construction	7	1	Exponential
Expressway	5	0.7	Linear
Railway	5	0.7	Linear
Road	3	0.5	Linear

The direct validation of the accuracy of the assessment results is a very challenging and difficult task due to the lack of well-recognized ground-truth habitat quality datasets. Nevertheless, it should be noted that both the FLUS and InVEST models adopted in this research are well-established and widely used methods with proven computational workflows and generally accepted input factors. The assessment factors in this study were selected with reference to related research in China [57], thereby ensuring the comparability of results.

The susceptibility of various land use classes to each threat factor exhibited notable variability. The susceptibility scores ranged from 0 (lowest susceptibility) to 1 (highest susceptibility). For example, the susceptibility of forest to road was 0.7, indicating a relatively high threat from the latter. Based on previous studies, the habitat resilience for different land use classes and their susceptibility to each threat factor were determined (Table 3) [11,13,21,26,61,62].

**Table 3.** Habitat resilience and threat factor susceptibility.

Class	Habitat Resilience	Susceptibility						
		Cropland	Urban Land	Rural Land	Other Construction	Expressway	Railway	Road
Cropland	0.4	0	0.5	0.4	0.2	0.3	0.2	0.2
Forest	1	0.5	0.7	0.6	0.4	0.6	0.6	0.7
Grassland	0.7	0.4	0.6	0.5	0.4	0.3	0.2	0.2
Water	0.9	0.6	0.9	0.7	0.6	0.6	0.5	0.6
Construction land	0	0	0	0	0	0	0	0
Unused land	0.2	0.2	0.3	0.3	0.3	0.2	0.2	0.1

### 2.2.3. FLUS Model

Liu et al. [36] put forth a future land use simulation (FLUS) approach by integrating a geographic modeling system with a neural network-based module. The FLUS method is able to accurately simulate land use evolution and project future changes. Given the

significant role of natural and socioeconomic variables in the land use evolution of China, key spatial factors were adopted based on related studies (Table 1) [15,32,34,40,48,63–65]. First, the probability of land use suitability was calculated on the basis of historical land use information. Then, the well-calibrated model was used for projecting future land use evolution in China by 2050.

### 3. Results

#### 3.1. Land Use Evolution

##### 3.1.1. Area Change in Land Use over 40 Years

Figure 2 illustrates the evolution of land use in China over the last four decades. Grassland, which consistently occupied the top position, showed a continuous decline, especially between 2010 and 2020. Forest coverage showed resilience despite initial challenges, exhibiting a recovery pattern in later years. The unused land remained relatively stable for three decades before showing a marked increase in the last period, indicating a growing trend of desertification and salinization. Among the other land use classes, cropland showed fluctuation patterns, while construction land exhibited consistent expansion throughout the study period.

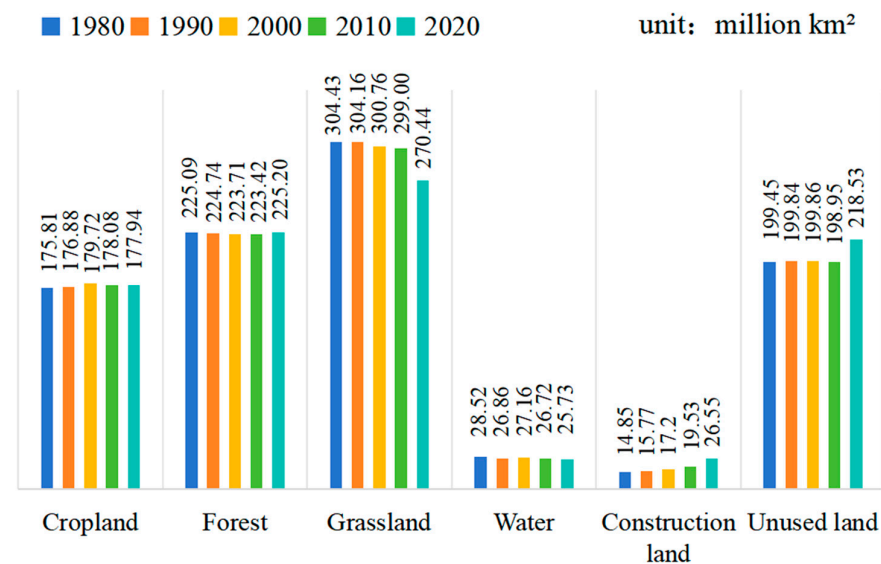


**Figure 2.** Evolution of land use area in China (1980–2020).

##### 3.1.2. Spatial Evolution of Land Use over 40 Years

Transformation matrices, trend state index, and annual average net change rate were calculated to further analyze the degree of land use evolution (Tables 4 and 5). The transformation matrices revealed several noteworthy patterns during the study period. The conversion dynamics remained relatively stable during 1980–2000, followed by significant changes during 2010–2020 with increased transformation intensity. An asymmetric conversion relationship was observed between cropland and forests, while construction land showed a distinct one-way transformation pattern. Notably, two critical transitions emerged: a sharp increase in grassland-to-unused land conversion during 2010–2020 after three decades of stability, and the diversification of construction land sources from predominantly cropland to multiple land classes. Although the water area maintained overall stability, it exhibited persistent minor transformations throughout the study period.

**Table 4.** Land use transformation matrices (1980–2020).

Period	Class	a	b	c	d	e	f
1980–1990	a	77.47%	11.80%	5.99%	1.21%	2.70%	0.81%
	b	9.13%	82.44%	7.34%	0.44%	0.29%	0.36%
	c	3.20%	5.45%	90.19%	0.30%	0.09%	0.76%
	d	8.79%	3.64%	1.92%	83.69%	0.89%	1.07%
	e	33.75%	4.75%	2.51%	2.26%	56.04%	0.68%
	f	0.49%	0.38%	1.03%	0.79%	0.02%	97.29%
1990–2000	a	86.52%	5.74%	4.69%	0.71%	2.88%	0.25%
	b	6.90%	87.19%	5.06%	0.23%	0.17%	0.44%
	c	3.52%	5.08%	85.88%	0.64%	0.12%	4.76%
	d	6.79%	1.93%	4.34%	80.32%	0.61%	6.01%
	e	16.04%	1.84%	1.73%	0.80%	79.37%	0.21%
	f	0.48%	0.63%	6.78%	0.83%	0.04%	91.23%
2000–2010	a	80.06%	9.13%	6.17%	1.21%	3.17%	0.26%
	b	7.14%	84.57%	7.10%	0.43%	0.51%	0.25%
	c	3.87%	5.43%	86.89%	0.40%	0.20%	3.22%
	d	7.19%	3.31%	4.27%	80.51%	1.85%	2.86%
	e	23.28%	4.84%	2.57%	1.93%	67.07%	0.31%
	f	0.50%	0.28%	4.87%	0.39%	0.08%	93.88%
2010–2020	a	62.59%	16.32%	9.51%	2.38%	8.04%	1.16%
	b	9.29%	80.92%	6.26%	0.90%	1.17%	1.46%
	c	6.44%	10.30%	63.31%	1.86%	0.64%	17.45%
	d	12.18%	4.47%	5.64%	70.09%	3.55%	4.07%
	e	31.64%	7.95%	4.53%	5.40%	49.43%	1.06%
	f	1.80%	1.53%	6.14%	1.79%	0.29%	88.45%
1980–2020	a	63.28%	15.33%	12.18%	2.03%	4.52%	2.66%
	b	7.33%	83.37%	6.97%	0.66%	0.40%	1.27%
	c	5.87%	9.39%	71.16%	1.47%	0.24%	11.87%
	d	9.51%	6.25%	4.43%	74.56%	2.02%	3.23%
	e	16.81%	8.88%	7.90%	3.15%	60.84%	2.43%
	f	0.69%	1.32%	4.43%	2.37%	0.07%	89.12%

Note: a—Cropland, b—forest, c—grassland, d—water, e—construction land, and f—unused land. Blue value indicates the percentage of land area that remained unchanged. Red value indicates the largest percentage of area for a given land use class that was transformed into another class.

**Table 5.** Area and proportion of different habitat degradation levels (1980–2020).

	Very Slight		Slight		Moderate		High		Severe	
	S	P (%)	S	P (%)	S	P (%)	S	P (%)	S	P (%)
1980	404.60	42.60	325.01	34.22	115.02	12.11	104.10	10.96	13.78	1.45
1990	404.81	42.62	326.11	34.33	110.87	11.67	103.66	10.91	16.04	1.69
2000	402.11	42.33	312.36	32.88	114.74	12.08	103.25	10.87	16.22	1.71
2010	394.30	41.51	310.86	32.73	111.40	11.73	105.29	11.08	17.09	1.80
2020	389.88	41.05	308.59	32.49	116.65	12.28	105.40	11.10	17.24	1.81
S <sub>net</sub>	−14.72	−13.64	−116.42	−15.05	1.63	1.42	1.30	1.25	3.46	25.11

Note: S means area (10,000 km<sup>2</sup>), P means proportion; S<sub>net</sub> means the net area change (S<sub>net</sub> = S<sub>end</sub> − S<sub>beginning</sub>); P<sub>SNet</sub> = S<sub>net</sub>/S<sub>beginning</sub> × 100%.

Between 1980 and 1990, the greatest net increase was seen in cropland, followed by construction and unused land. Construction land exhibited the highest trend index (0.07) and net change rate (0.62%), indicating a rapid expansion over the past 10 years. Between 1990 and 2000, forests and grassland declined, while cropland and construction land expanded most notably (0.16% and 0.90%, respectively). Between 2000 and 2010, construction

land continued to expand significantly, while other land use classes decreased, with water experiencing the largest decline ( $-0.16\%$ ). Between 2010 and 2020, construction land experienced its peak expansion ( $3.60\%$ ), while grassland continued to decline ( $-285,600 \text{ km}^2$ ,  $-0.96\%$ ). Cropland also decreased, but at a slower rate ( $-15,000 \text{ km}^2$ ), while forest and unused land expanded ( $0.08\%$  and  $0.98\%$ , respectively). In summary, construction land has seen the most dramatic growth over the past 40 years, in contrast to the steady decline in grassland and water. Unused land expanded throughout the study period, except for a slight decrease during 2000–2010. The most rapid expansion occurred between 2010 and 2020. Cropland and forest land have maintained a relatively constant level.

### 3.1.3. Projection of Land Use Evolution by 2050

Given that the FLUS model was designed to be calibrated and simulated using only the most recent two years of data, the land use projections for 2050 were based on the data from the 2010 to 2020 period. Specifically, this research began with an investigation of land use information from 2010. The suitability probability of every land use class was computed using the FLUS method's neural network module, and then the land use evolution during 2010–2020 was simulated. The modeling results were validated against the real land use information in 2020. A satisfactory kappa coefficient of 0.736 was yielded, demonstrating high simulation accuracy. This value is higher than the kappa coefficient (0.67) obtained by the original FLUS research for China's national simulation [36], and the kappa coefficients (0.76 in 2015) and (0.72 in 2018) obtained by a regional application in Hengyang City [66]. Our model shows comparable accuracy despite covering a much larger geographical extent. This validation supports the reliability of the FLUS model in simulating future land use evolution at the national scale.

Subsequently, a Markov Chain approach was employed for projecting the area change in land use by 2050. Finally, we projected the land use status in 2050 with the support of the well-calibrated model (Figure 3).

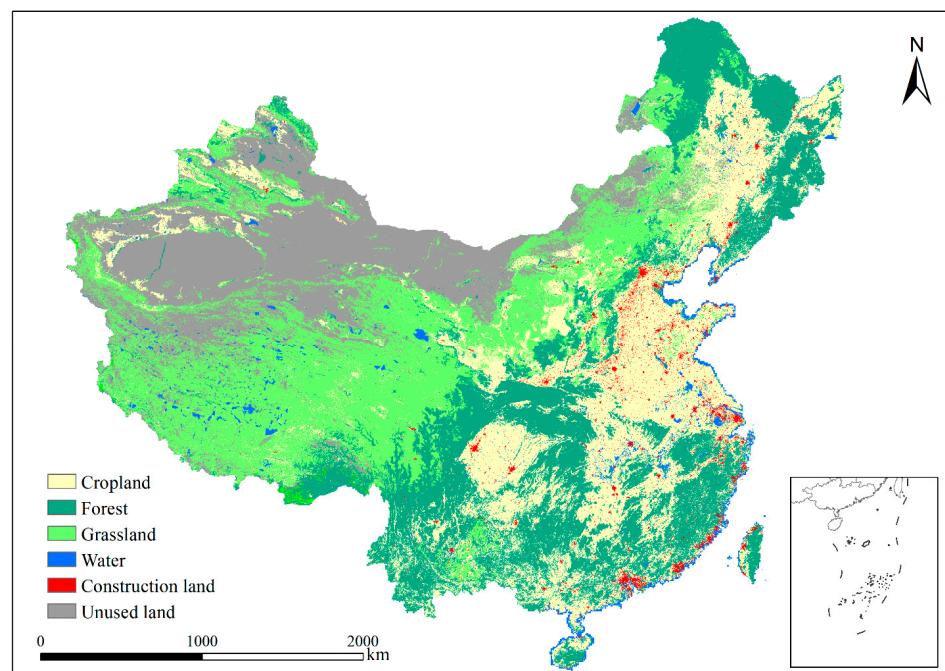


**Figure 3.** Land use projection results in 2050.

The spatial analysis reveals several critical transformation patterns. The reduction in grassland is predominantly concentrated in northwestern China's ecologically fragile regions, while construction land expansion exhibits a continuous sprawl pattern along the



eastern coastal areas. Notably, there is a high spatial correlation between grassland loss and unused land expansion, suggesting potential ecological degradation risks. Although unused land shows the largest absolute increase, construction land demonstrates the highest annual rate of change (1.90%), indicating that urbanization remains the dominant driving force. The reciprocal relationship between grassland and forests decline suggests a structural transformation of ecosystems. Furthermore, the simultaneous expansion of construction and unused land, coupled with the reduction in ecological land (grassland and forests), forms a self-reinforcing trend that may accelerate the deterioration of regional ecosystem services.

### 3.2. Habitat Quality Change

#### 3.2.1. Spatiotemporal Change in Habitat Degradation

The average habitat degradation degree from 1980 to 2020 was evaluated through the InVEST method. As illustrated in Figure 4, the temporal pattern reveals three distinct phases of habitat degradation. The sharp increase in the 1980s coincided with rapid economic development, followed by a relatively stable period in the 1990s despite continued degradation. While the acceleration resumed in the 2000s, the recent plateauing trend suggests a potential transition in environmental pressure, though at persistently high levels.

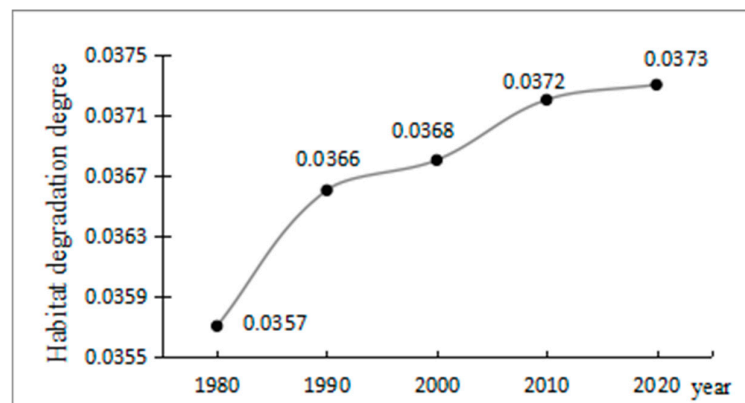


**Figure 4.** Change in the average habitat degradation degree (1980–2020).

Subsequently, the degradation degree was classified as five levels through the natural breaks: very slight (0–0.015), slight (0.015–0.03), moderate (0.03–0.09), high (0.09–0.17), and severe (0.17–0.34) (Figure 5). Table 5 presents the area and proportion of each level. Over the last four decades, the analysis reveals a concerning shift in habitat quality distribution. The systematic decrease in better-preserved habitats alongside the expansion of degraded areas suggests a continuous environmental pressure pattern. The most notable transformation occurred in the conversion from very slightly degraded to more severe levels, indicating a gradual erosion of excellent-quality habitats.

Over the last four decades, China’s habitat degradation has generally exhibited a west-to-east gradient of increasing severity, closely aligned with the country’s topographic variation. The spatial pattern of habitat degradation demonstrates a clear association with China’s development patterns. A distinct degradation gradient emerges from the relatively preserved western plateaus to the intensively developed eastern regions, aligned with the nation’s economic geography. The spatial concentration of severe degradation is particularly evident in urban agglomerations and their surrounding areas, where the urban–rural transition zones show the most significant habitat degradation.

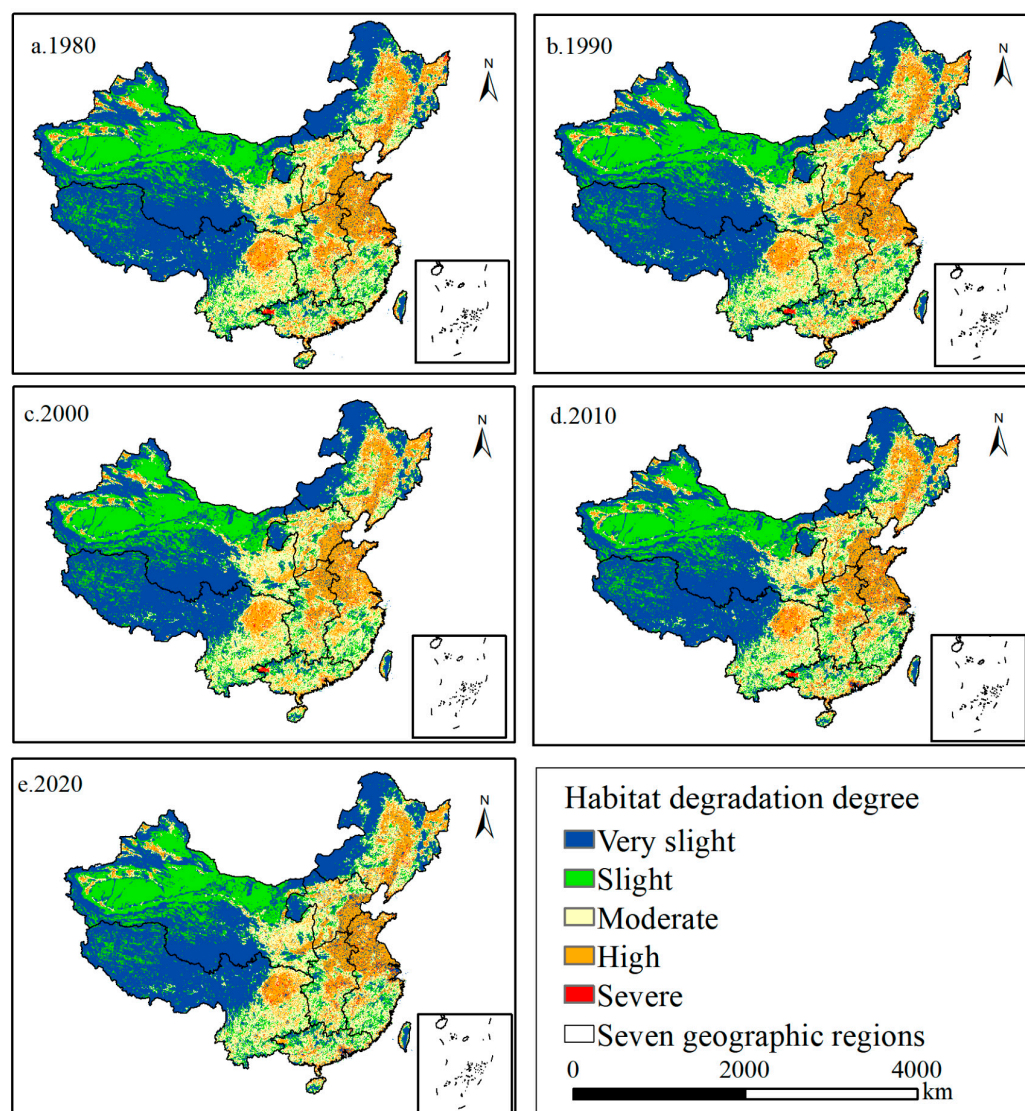


Figure 5. Spatial pattern of habitat degradation degree (1980–2020).

### 3.2.2. Spatiotemporal Change in Habitat Quality

Next, the average habitat quality indices in China from 1980 to 2020 (Figure 6) reveal a decreasing tendency in habitat quality. This decline was initially slight over the first two decades, followed by a sharp decrease between 2000 and 2010. A slight improvement was observed after 2010, but overall, the habitat quality in China has declined during the last four decades.

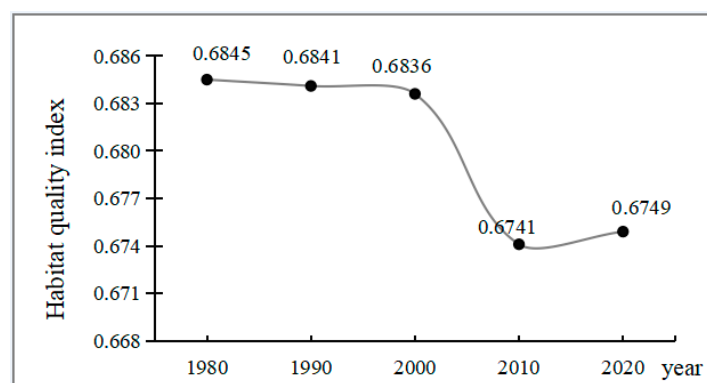
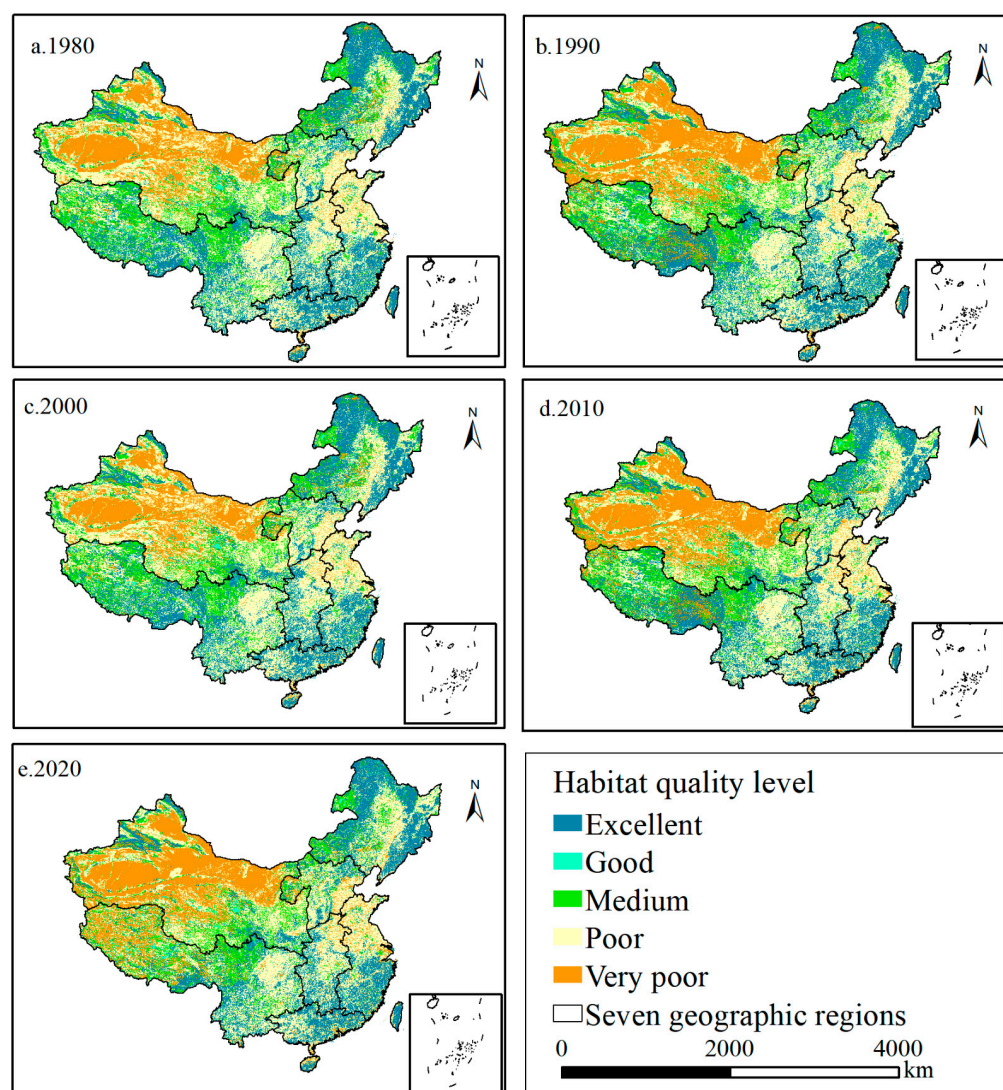


Figure 6. Average habitat quality indices (1980–2020).

The natural break approach was utilized for classifying the habitat quality index into five levels (Table 6 and Figure 7). The spatial pattern of habitat quality has changed significantly over the past 40 years, with the largest values in the eastern and southern regions and the smallest in the northwest. The good-quality habitats were initially concentrated in Inner Mongolia and the Qinghai–Tibet Plateau. However, in the last decade, a small part of the Qinghai–Tibet Plateau has dropped from good to medium quality. The Heilongjiang Basin, the Greater Khingan Range, the Yunnan–Guizhou Plateau, and the southern Yangtze River region, characterized by lush vegetation and developed water systems, had excellent habitat quality. Moderate-quality habitats were often adjacent to excellent habitats, such as the Northeast Plain, North China Plain, and Pearl River Delta, which were dominated by cropland. Conversely, habitats with very poor quality were concentrated in the Tarim and Junggar Basins, with the remaining habitats dispersed within urban agglomerations. Poor-quality habitats were primarily located in the northwest, often adjacent to those with very poor quality. Overall, China’s habitat quality was closely linked to land use, terrain, and resource availability.



**Figure 7.** Spatial pattern of habitat quality levels (1980–2020).

**Table 6.** Area and percentage of different habitat quality levels (1980–2020).

	Excellent		Good		Medium		Poor		Very Poor	
	S	P (%)	S	P (%)	S	P (%)	S	P (%)	S	P (%)
1980	235.62	24.85	158.22	16.69	284.81	30.04	78.09	8.24	191.26	20.18
1990	233.06	24.58	157.44	16.60	287.72	30.34	76.72	8.09	193.26	20.38
2000	229.32	24.17	155.14	16.35	289.76	30.53	78.16	8.24	193.59	20.40
2010	225.47	23.80	153.60	16.21	288.75	30.48	81.41	8.59	195.25	20.61
2020	224.05	23.62	146.64	15.46	266.35	28.08	85.39	9.00	224.19	23.63
S <sub>net</sub>	−11.56	−4.91	−11.58	−7.32	−18.45	−6.48	7.30	9.35	32.93	17.22

Over the 40-year period, the size of excellent-, good-, and medium-quality habitats all decreased. This simultaneous decrease in medium-quality habitats and the expansion of very poor habitats suggests a concerning polarization trend. Despite the overall declining trend, certain regions like the Greater Khingan Range maintained their excellent quality, suggesting the effectiveness of ecological protection in these areas. These trends, along with the patterns observed in Figures 6 and 7, indicate an overall decline in China’s average habitat quality from good to medium.

Next, a transformation matrix analysis was performed for quantifying the spatial changes in habitat quality levels (Table 7). The transformation outcomes were classified into three categories: increased, decreased, and unchanged habitat quality (Figure 8). Overall, most habitats exhibited no discernible change in quality, but the habitats displaying a decline in quality exceeded those demonstrating an improvement. Unchanged habitats accounted for the largest proportion, concentrated in the Tarim Basin, Sichuan Basin, and Inner Mongolia Plateau. Increased quality habitats (blue value in Table 7) comprised the study area, primarily located around northwestern and southwestern zones, with the remainder dispersed throughout China. In contrast, decreased quality habitats (red value in Table 7) comprised the study area, mostly distributed in small clusters in alpine regions such as the Junggar Basin, the Qinghai–Tibet Plateau, and coastal urbanized zones.

Furthermore, substantial changes were observed across habitats with varying quality levels. The excellent habitats were the most stable, remaining unchanged, degrading to good quality, and a minor proportion degrading to medium, poor, and very poor quality. The transformation showed a “jumping” pattern of degradation, with habitats often degrading beyond the adjacent quality level. Good-quality habitats were particularly vulnerable, with a significant proportion experiencing severe degradation. Notably, medium-quality habitats showed the highest instability, suggesting that they may serve as a critical threshold in the degradation process. Transformation patterns showed a “one-way” degradation tendency, with very poor habitats showing the greatest resistance to quality improvement.

**Table 7.** Habitat quality transformation matrix (1980–2020).

	Quality Level	2020				
		Excellent	Good	Medium	Poor	Very Poor
1980	Excellent	84.73%	10.51%	2.22%	1.87%	0.67%
	Good	4.60%	61.01%	9.60%	36.58%	6.33%
	Medium	0.62%	9.46%	57.78%	14.39%	18.41%
	Poor	0.54%	3.93%	8.91%	62.37%	10.38%
	Very poor	0.35%	2.67%	13.96%	14.10%	71.41%

Note: Blue value indicates the percentage of area with increased habitat quality. Red value indicates the percentage of area with decreased habitat quality.

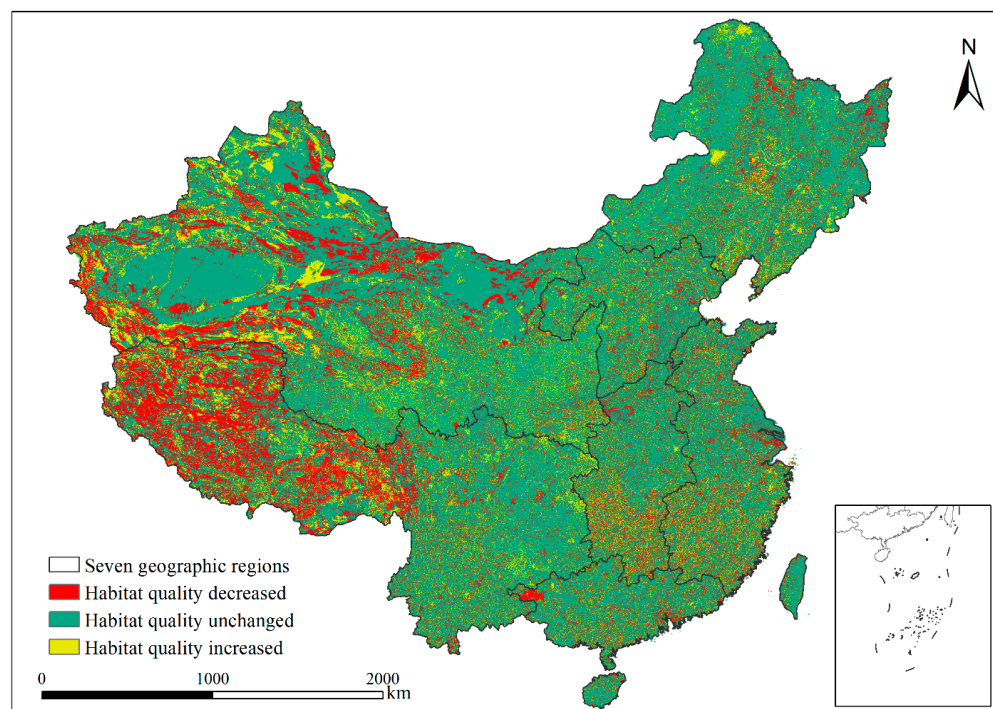


**Figure 8.** Transformation in habitat quality levels (1980–2020).

### 3.2.3. Habitat Quality Change Across Different Land Use Classes

Given the considerable variation in the development characteristics and protection levels of the different land use classes, a further investigation was conducted to identify the underlying cause of the change in habitat quality across the different land use classes (Figure 9). Despite relative stability in cropland habitat quality over the past 40 years, the slight improvement suggests successful agricultural land management practices. In addition, forest land is the dominant land use class in regions with excellent and good habitat quality. More notably, forest quality showed a concerning polarization trend, with accelerated degradation particularly after 2010, suggesting that a potential ecological threshold was reached.

Moreover, the quality of grasslands showed a critical tipping point in 2010, after which all quality levels showed a significant decline, indicating a cascading degradation process. Meanwhile, unlike other land classes, water bodies showed fluctuating quality patterns rather than unidirectional degradation, with relative stability in excellent- and good-quality areas after 2010, possibly reflecting the effectiveness of water resource management measures. The synchronized expansion of construction land and the degradation of unused land quality during 2010–2020 reveal the compound effects of urbanization on habitat quality. In summary, forests and grassland are important sources of excellent-quality habitats in China, and the interconnected degradation patterns across different land use classes suggest a complex web of ecological interactions that warrant immediate attention.

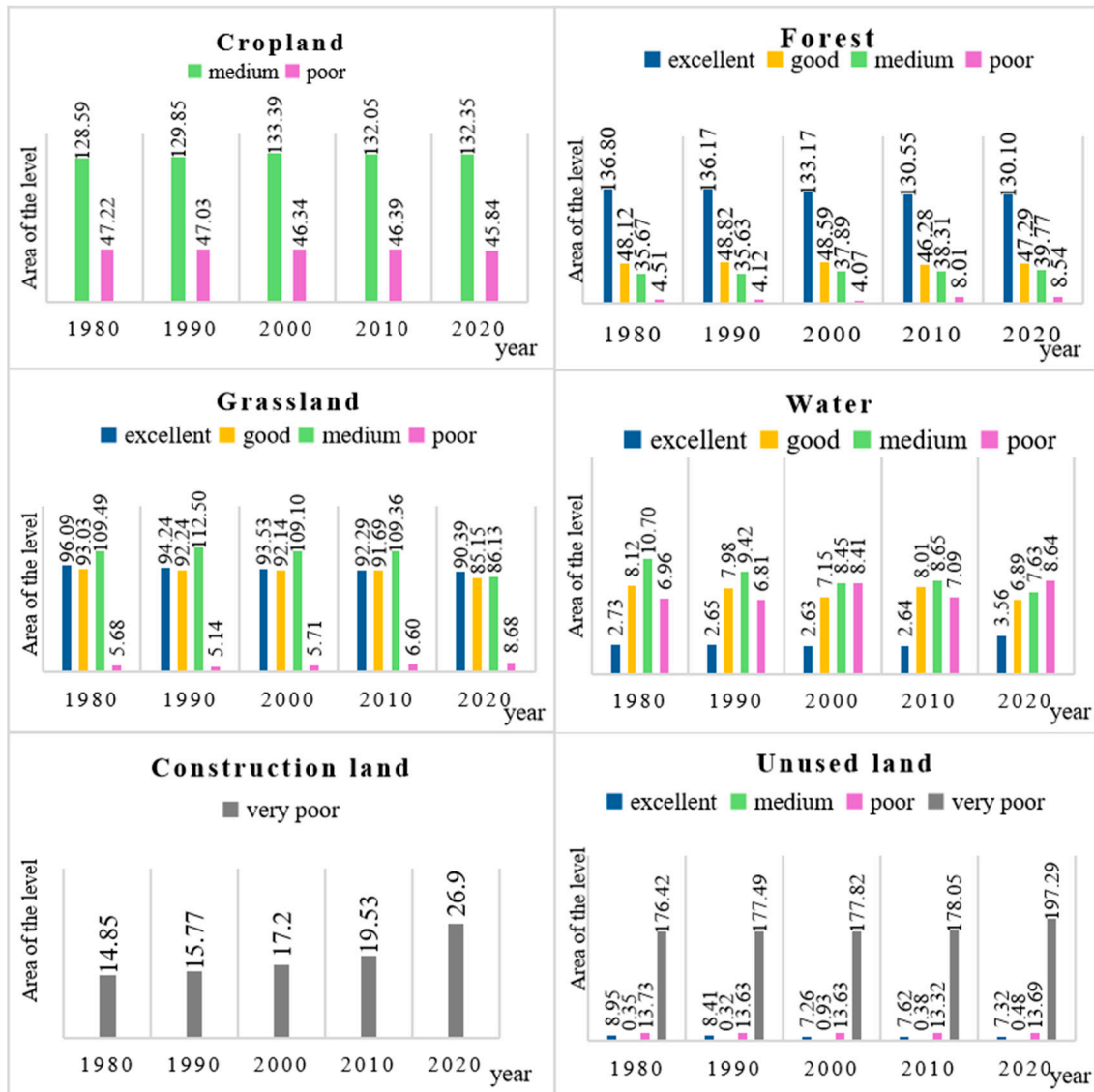


Figure 9. Area of habitat quality levels by land use classes (unit: 10,000 km<sup>2</sup>).

### 3.2.4. Future Habitat Quality Projection

The InVEST method was employed for assessing habitat quality in accordance with the land use projection results in 2050 (Figure 10). While acknowledging the uncertainty of future changes to the transport network, we focused on major roads as they represented the primary infrastructure impact on habitat quality, an approach validated by previous research.

Our analysis shows a decline in excellent- and good-quality habitats within natural areas, while very poor-quality habitats will increase around urban and high-altitude zones. The Qinghai–Tibet Plateau demonstrated enhanced habitat quality. From 2020 to 2050, excellent habitats displayed an “island effect” in coastal areas, while medium-quality habitats formed a belt-like pattern across central China.

We used the aforementioned methodology to analyze the habitat quality levels in 2050 (Table 8). The 2050 projection reveals concerning patterns in different land use classes. Cropland will be dominated by medium-quality habitats, with no excellent- or good-quality areas remaining. Unused land showed polarization between minimal good-quality areas and extensive poor-quality regions, indicating challenges for ecological preservation.

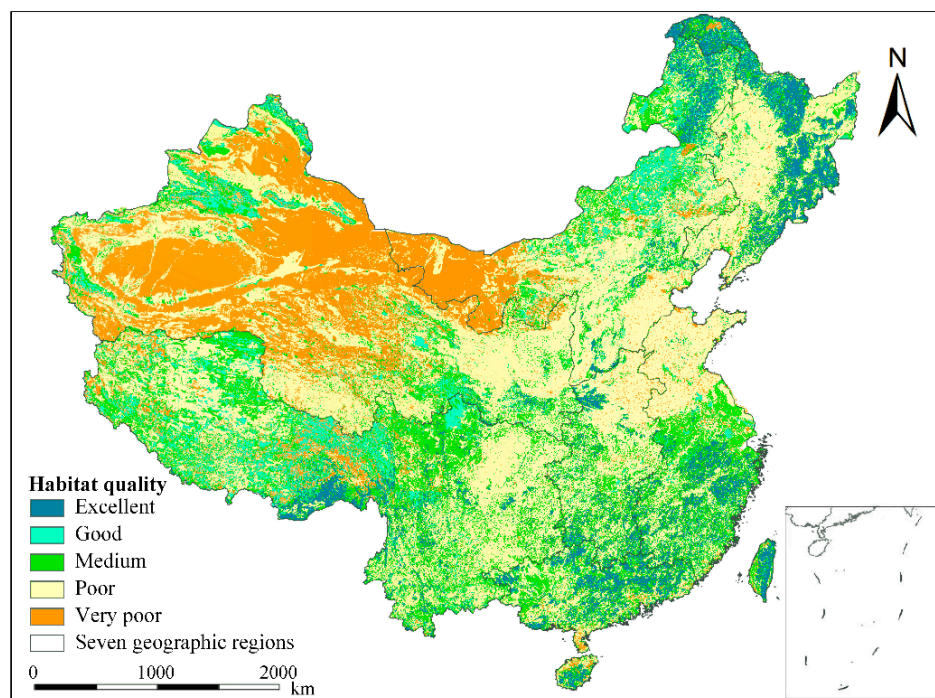


**Figure 10.** Projected habitat quality in China in 2050.

**Table 8.** Area of different habitat quality levels in 2050 (unit: 10,000 km<sup>2</sup>).

	Cropland	Forest	Grassland	Water	Construction Land	Unused Land	Sum
Excellent	0	120.77	70.76	4.12	0	0	195.65
Good	0	43.97	76.54	6.54	0	6.12	133.17
Medium	135.89	30.74	79.15	7.41	0	0	253.19
Poor	48.79	16.00	7.21	8.92	0	20.12	101.04
Very poor	0	0	0	0	41.66	219.54	261.20

This projected degradation of habitat quality poses a significant threat to biodiversity, particularly in the urban–rural transition zones, where habitat fragmentation is most severe. The conversion of excellent- and good-quality habitats could have a significant impact on species migration corridors and ecosystem stability, with forests and grasslands experiencing the most significant losses in terms of both area and quality. These changes are primarily driven by urban expansion and insufficient ecological restoration.

## 4. Discussion

### 4.1. Causes of Habitat Quality Degradation

Over the last forty years, China has undergone a notable decline in habitat quality, primarily driven by unreasonable land use evolution. Construction land continued to encroach upon key land use classes involving forests, grassland, and water. The severely and highly degraded habitats were concentrated in the urban agglomerations and urban–rural fringes of southeastern China, which have undergone significant urbanization and industrialization. The anthropogenic pressures have significantly altered land use patterns, with extensive land use becoming a prominent issue in these zones [57,67,68].

Over the past four decades, China’s economic development policies have, to some extent, failed to adequately address the importance of ecological and environmental protection. In order to achieve economic growth and catch up with developed countries, some regions have adopted a development pattern that involves a trade-off between high resource consumption and high environmental costs on the one hand, and economic

prosperity on the other. This short-sighted economic strategy has resulted in long-term, cumulative consequences for the ecological environment. Notably, this has resulted in substantial urbanization and habitat degradation in regions such as the Pearl River Delta and the Yangtze River Delta [69]. Despite national government initiatives to promote habitat restoration through policies such as urban development boundaries and ecological compensation, challenges persist, particularly in the context of legal frameworks for habitat conservation, which remain inadequate and lack cross-sectoral coordination [70]. Grassland has experienced the most substantial decline over the past 40 years, with a large proportion being converted to unused land. The degradation of grasslands, caused by factors such as overgrazing, overcultivation, and irrational irrigation, has resulted in land siltation and a reduction in pasture production. Furthermore, the deterioration of grasslands has contributed to an increase in the frequency and intensity of natural disasters, including sandstorms and dust storms. The cascading effects of grassland degradation extend beyond local ecosystems, creating interconnected environmental challenges across regions. This highlights the need for an integrated approach to habitat conservation that considers both the direct and indirect impacts of land use changes.

Historically, cropland and forests have maintained a mutually beneficial relationship in China. The largest type of land transferred from cropland is forests, which is also the largest source of transfers from cropland. However, the increasing pressure for food has caused the excessive conversion of ecological resources, including forests and grassland, into cropland. This has resulted in adverse consequences such as soil erosion, forest cover loss, and land desertification [2,71,72]. Some farmers have exacerbated the issue by clearing forests and cropland to plant high-profit fruit trees. Recent studies using advanced remote sensing and GIS technologies have revealed complex patterns of forest–cropland interactions. These patterns suggest that successful habitat restoration requires not only increasing forest cover but also maintaining landscape connectivity and ecological corridors [73–75]. Additionally, the quality of restored habitats varies significantly based on local environmental conditions and restoration approaches [76,77]. This highlights that maintaining or increasing forest cover alone does not guarantee improved habitat quality, and underscores the importance of considering other factors, such as landscape connectivity and habitat heterogeneity, in conservation efforts.

The proportion of water, although relatively small, has also been declining. First, the accelerated disappearance of lakes can be attributed to long-term land reclamation and overfishing [78–80]. Second, a significant proportion of wetland has been damaged and degraded, resulting in the transformation of these ecosystems into barren beaches. Third, the excessive exploitation and irrational utilization of water resources have resulted in the emergence of water scarcity issues, including the desiccation of rivers and the reduction in reservoir levels. This not only affects the productivity and well-being of individuals but also contributes to the deterioration of the ecological environment. Furthermore, the implementation of water conservation and waterway regulation projects has inadvertently contributed to ecosystem degradation and water pollution, resulting in a decline in water quality [81–83]. The most striking phenomenon is the expansion of unused land, which consists mainly of poor- and very poor-quality habitats. Particularly, the very poor-quality habitats, which were concentrated in the Tarim and Junggar Basins and were characterized by sandy, saline–alkaline, and bare soils, have increased significantly over the last decade due to low rainfall and poor soil quality [84–87].

#### 4.2. Countermeasures to Improve Habitat Quality

First, the optimization of land use patterns and the strict adherence to land use quotas are of paramount importance. Governments must rigorously enforce policies to safeguard



high-quality cropland and return low-quality cropland to forests, ensuring an optimal balance between these resources [88–90]. To safeguard high-quality cropland, it is crucial to enhance the system for balancing cropland occupation and replenishment. Given the moderate quality of cropland habitats, promoting organic fertilization can improve soil health without the necessity of expanding cropland [91–93]. The effective protection of dominant habitats (e.g., forests, grassland, and water) is vital to prevent land degradation. Regarding construction land, efficient and intensive land use patterns should be implemented. Additionally, assessing land carrying capacity and suitability can reveal the current state of regional land use, thereby promoting ecological balance and enhancing land use efficiency [63,94–96].

Second, it is also essential to stabilize high-quality habitats and restore degraded habitats. In high-quality habitats, enhancing resilience to climate change is crucial for strengthening regional ecosystems and enriching biodiversity [97–99]. Currently, China's ecological restoration efforts can be categorized into three main types: restoration, regulation, and reconstruction [64,100–102]. A variety of restoration methods should be employed based on specific habitat conditions. In habitats with slight degradation and good quality (e.g., the Qinghai–Tibet Plateau), the focus is on facilitating the natural recovery of ecosystems, supplemented by artificial restoration projects. Habitats with high degradation and average habitat quality, such as the middle reaches of the Changjiang Plain, rely primarily on land restoration and ecological engineering to restore regional ecosystem functionality. For habitats with severe degradation and poor quality, such as the Loess Plateau, large-scale ecological reconstruction is necessary.

Third, it is essential to establish a robust partnership between governments and citizens for advancing conservation initiatives and raising public awareness of ecological issues. This requires a shift from managing individual regions in isolation to a more integrated approach that recognizes the interdependence of diverse ecological elements across China [103–105]. This includes optimizing China's land use patterns from a macro perspective and promoting the systematic restoration and holistic protection of the environment [106–108]. Raising public awareness is paramount in this endeavor. Governments should educate citizens about environmental laws and promote habitat conservation through documentaries and case studies [109,110]. By fostering ecological awareness, citizens will be empowered to consciously fulfill their environmental protection obligations. This collaborative effort between governments and citizens is essential for achieving more effective conservation outcomes.

#### 4.3. Strengths and Limitations

The limited regional scope of previous studies has constrained our understanding of habitat quality changes and interregional interactions. For example, Ren et al. [111] focused specifically on the influence of threat factors within a medium-sized region, which may result in an underestimation of the role of inter-regional factors. In addition, the findings of studies conducted in medium- and small-sized regions may be constrained in their generalizability. For example, Hack et al. [112] observed that the impacts of threat factors in the Pochote River Basin exhibited considerable variation from areas in close proximity to the city center to those situated downstream. This finding highlights the limitations of localized studies in capturing broader ecological processes and inter-regional interactions.

Regional protection strategies must be coordinated at the national scale to effectively influence habitat quality and inform conservation strategies. In particular, Sallustio et al. [113] conducted a nationwide research project on habitat quality in Italy. This study successfully identified priority conservation areas and supported large-scale strategic conservation measures, which demonstrates the benefits of national-scale assessment. In consideration

of the findings of the national-scale assessment presented in this study, we propose the following countermeasures for enhancing habitat quality with the objective of optimizing land use patterns and achieving sustainable development in China.

In addition, long-term research provides a comprehensive understanding of habitat quality trends, particularly given the complex and dynamic nature of ecosystems. Long-term research, on the other hand, is much more appropriate for determining the direction and rate of change in habitat quality by analyzing and comparing data over several decades. This provides a more reliable foundation for large-scale ecological conservation and management.

This research has several limitations that warrant further investigation. First, the assessment of habitat quality should incorporate a wider range of threat factors to enhance the rationality of factor selection. Second, this research considered solely the effect of land use on habitat quality, neglecting other essential ecological factors including soil and water conservation, the establishment of protected areas, and forest restoration processes due to data availability. Third, while distinguishing between planted and natural forests would be advantageous for a more comprehensive examination of habitat quality, these forest categories were not distinguished in this study due to data limitations. Existing national land cover datasets lack the necessary detail to consistently and accurately distinguish between these forest categories. Future research should incorporate multiple data sources to enable finer-scale forest classification. Finally, the large study area and model complexity led to difficulties in data collection and potential differences between projected and actual land use results. Future research could integrate additional spatial factors and policy conditions into multi-scenario simulations.

Conservation incentives should be incorporated into future ecological projections for 2050. Policy instruments such as ecological compensation and green credits can promote sustainable practices in agriculture, forestry, and fisheries. Additionally, expanding protected areas and promoting afforestation could enhance biodiversity conservation. These factors would provide valuable insights for environmental protection measures.

## 5. Conclusions

This study analyzed the evolution of habitat quality in China over the last forty years and projected future quality levels for 2050. The results revealed a graded spatial pattern of habitat degradation across different terrain levels, with severe degradation in first-level terrain, moderate degradation in second-level terrain, and slight degradation in third-level terrain. The FLUS model (kappa coefficient = 0.736) projected the significant encroachment of construction land upon forests and grassland by 2050, indicating an urgent need for targeted conservation measures.

Based on our findings, the following conservation strategies are recommended to enhance and safeguard habitat quality. First, natural recovery should be prioritized for high-quality habitats (e.g., Qinghai–Tibet Plateau) while enhancing climate resilience through habitat protection. Second, land restoration and ecological engineering should be implemented in moderately degraded areas (e.g., Changjiang Plain), with a focus on organic fertilization to improve soil health. Third, ecological restoration and the strict control of urban sprawl should be implemented in severely degraded regions (e.g., Loess Plateau).

The successful implementation of these strategies requires the strengthening of land use quotas, the development of integrated conservation approaches, and the enhancement of government–citizen partnerships through environmental education. Future research should incorporate conservation incentives and ecological compensation mechanisms to better support China's sustainable development goals.

**Author Contributions:** Writing—Original Draft, Formal Analysis, Y.C.; Investigation, Validation, F.Z.; Supervision, Project Administration, J.L. All authors have read and agreed to the published version of the manuscript.

**Funding:** This research was funded by the Humanities and Social Sciences Research Program of the Ministry of Education of China (Grant No. 23YJCZH125), the Guangdong Basic and Applied Basic Research Foundation (Grant No. 2023A1515030300), and the Guangdong Philosophy and Social Science Foundation (Grant No. GD23XSH11).

**Institutional Review Board Statement:** Not applicable.

**Informed Consent Statement:** Not applicable.

**Data Availability Statement:** The data presented in this study are available on request from the corresponding author.

**Conflicts of Interest:** The authors declare no conflicts of interest.

## References

- Jafino, B.A.; Kwakkel, J.H.; Klijn, F.; Dung, N.V.; van Delden, H.; Haasnoot, M.; Sutanudjaja, E.H. Accounting for Multisectoral Dynamics in Supporting Equitable Adaptation Planning: A Case Study on the Rice Agriculture in the Vietnam Mekong Delta. *Earth's Future* **2021**, *9*, e2020EF001939. [\[CrossRef\]](#)
- Liu, X.; Huang, Y.; Xu, X.; Li, X.; Li, X.; Ciais, P.; Lin, P.; Gong, K.; Ziegler, A.D.; Chen, A.; et al. High-spatiotemporal-resolution mapping of global urban change from 1985 to 2015. *Nat. Sustain.* **2020**, *3*, 564–570. [\[CrossRef\]](#)
- Liu, Y.; He, Q.; Tan, R.; Liu, Y.; Yin, C. Modeling different urban growth patterns based on the evolution of urban form: A case study from Huangpi, Central China. *Appl. Geogr.* **2016**, *66*, 109–118. [\[CrossRef\]](#)
- Li, G.; Sun, S.; Fang, C. The varying driving forces of urban expansion in China: Insights from a spatial-temporal analysis. *Landsc. Urban Plan.* **2018**, *174*, 63–77. [\[CrossRef\]](#)
- Fu, H.; Zhao, S.; Liao, C. Spatial governance of Beijing-Tianjin-Hebei urban agglomeration towards low-carbon transition. *China Agric. Econ. Rev.* **2022**, *14*, 774–798. [\[CrossRef\]](#)
- Feng, H.; Wang, S.; Zou, B.; Nie, Y.; Ye, S.; Ding, Y.; Zhu, S. Land use and cover change (LUCC) impacts on Earth's eco-environments: Research progress and prospects. *Adv. Space Res.* **2023**, *71*, 1418–1435. [\[CrossRef\]](#)
- Feng, Y.; Wu, P.; Tong, X.; Li, P.; Wang, R.; Zhou, Y.; Wang, J.; Zhao, J. The effects of factor generalization scales on the reproduction of dynamic urban growth. *Geo-Spat. Inf. Sci.* **2022**, *25*, 457–475. [\[CrossRef\]](#)
- Chen, Y.; Zhao, S.; Pei, L. Comparing the warming effects of different urban forms under projected climate change in China's Guangdong-Hong Kong-Macau Greater Bay Area. *Urban Clim.* **2024**, *53*, 101824. [\[CrossRef\]](#)
- Jiang, P.; Li, M.; Sheng, Y. Spatial regulation design of farmland landscape around cities in China: A case study of Changzhou City. *Cities* **2020**, *97*, 102504. [\[CrossRef\]](#)
- Guo, Y.; Tang, J.; Liu, H.; Yang, X.; Deng, M. Identifying up-to-date urban land-use patterns with visual and semantic features based on multisource geospatial data. *Sustain. Cities Soc.* **2024**, *101*, 105184. [\[CrossRef\]](#)
- An, Y.; Liu, S.; Sun, Y.; Shi, F.; Zhao, S.; Liu, Y.; Li, M. A partitioning approach for regional sustainability based on economic development indicators and ecological values for China. *J. Nat. Conserv.* **2022**, *67*, 126179. [\[CrossRef\]](#)
- Kong, X.; Zhou, Z.; Jiao, L. Hotspots of land-use change in global biodiversity hotspots. *Resour. Conserv. Recycl.* **2021**, *174*, 105770. [\[CrossRef\]](#)
- Zhang, Z.; Gong, J.; Plaza, A.; Yang, J.; Li, J.; Tao, X.; Wu, Z.; Li, S. Long-term assessment of ecological risk dynamics in Wuhan, China: Multi-perspective spatiotemporal variation analysis. *Environ. Impact Assess. Rev.* **2024**, *105*, 107372. [\[CrossRef\]](#)
- Huang, Q.; Liu, Z.; He, C.; Gou, S.; Bai, Y.; Wang, Y.; Shen, M. The occupation of cropland by global urban expansion from 1992 to 2016 and its implications. *Environ. Res. Lett.* **2020**, *15*, 084037. [\[CrossRef\]](#)
- Li, X.; Zhou, Y.; Gong, P. Diversity in global urban sprawl patterns revealed by Zipfian dynamics. *Remote Sens. Lett.* **2023**, *14*, 565–575. [\[CrossRef\]](#)
- Vach, M.; Vachová, P.; Walmsley, A.; Berka, M.; Albert, J.; Cienciala, E.; Braun Kohlová, M.; Máca, V.; Melichar, J. Stochastic evaluation of restoration procedures on postmining land areas using a game theory approach. *Land Degrad. Dev.* **2022**, *33*, 484–496. [\[CrossRef\]](#)
- Niu, J.; Tang, W.; Xu, F.; Zhou, X.; Song, Y. Global Research on Artificial Intelligence from 1990–2014: Spatially-Explicit Bibliometric Analysis. *ISPRS Int. J. Geo-Inf.* **2016**, *5*, 66. [\[CrossRef\]](#)
- Li, H.; Peng, Y.; Li, M.; Zhuang, Y.; He, X.; Lin, J. Analyzing spatial patterns and influencing factors of different illegal land use types within ecological spaces: A case study of a fast-growing city. *J. Clean. Prod.* **2023**, *424*, 138883. [\[CrossRef\]](#)

19. Ke, X.; van Vliet, J.; Zhou, T.; Verburg, P.H.; Zheng, W.; Liu, X. Direct and indirect loss of natural habitat due to built-up area expansion: A model-based analysis for the city of Wuhan, China. *Land Use Policy* **2018**, *74*, 231–239. [[CrossRef](#)]
20. Liao, J.; Tang, L.; Shao, G. Coupling Random Forest, Allometric Scaling, and Cellular Automata to Predict the Evolution of LULC under Various Shared Socioeconomic Pathways. *Remote Sens.* **2023**, *15*, 2142. [[CrossRef](#)]
21. Wang, A.; Zhang, M.; Kafy, A.A.; Tong, B.; Hao, D.; Feng, Y. Predicting the impacts of urban land change on LST and carbon storage using InVEST, CA-ANN and WOA-LSTM models in Guangzhou, China. *Earth Sci. Inform.* **2023**, *16*, 437–454. [[CrossRef](#)]
22. Li, M.; Luo, H.; Qin, Z.; Tong, Y. Spatial-Temporal Simulation of Carbon Storage Based on Land Use in Yangtze River Delta under SSP-RCP Scenarios. *Land* **2023**, *12*, 399. [[CrossRef](#)]
23. Tian, C.; Pang, L.; Yuan, Q.; Deng, W.; Ren, P. Spatiotemporal Dynamics of Ecosystem Services and Their Trade-Offs and Synergies in Response to Natural and Social Factors: Evidence from Yibin, Upper Yangtze River. *Land* **2024**, *13*, 1009. [[CrossRef](#)]
24. Herischian, M.; Mahmoudzadeh, H.; Ghorbani, R. Investigating the effect of the cooling ecosystem service of urban green infrastructure on the mitigating of environmental heat load and energy efficiency in the metropolitan of Tabriz. *Geogr. Urban Plan. Res.* **2024**, *11*, 175–203. [[CrossRef](#)]
25. Xu, C.; Chen, X.; Yu, Q.; Avirmed, B.; Zhao, J.; Liu, W.; Sun, W. Relationship between ecological spatial network and vegetation carbon use efficiency in the Yellow River Basin, China. *GISci. Remote Sens.* **2024**, *61*, 2318070. [[CrossRef](#)]
26. Cheng, W.; Ma, C.; Li, T.; Liu, Y. Construction of Ecological Security Patterns and Evaluation of Ecological Network Stability under Multi-Scenario Simulation: A Case Study in Desert–Oasis Area of the Yellow River Basin, China. *Land* **2024**, *13*, 1037. [[CrossRef](#)]
27. He, Q.; Zhou, J.; Tan, S.; Song, Y.; Zhang, L.; Mou, Y.; Wu, J. What is the developmental level of outlying expansion patches? A study of 275 Chinese cities using geographical big data. *Cities* **2020**, *105*, 102395. [[CrossRef](#)]
28. Liang, X.; Guan, Q.; Clarke, K.C.; Liu, S.; Wang, B.; Yao, Y. Understanding the drivers of sustainable land expansion using a patch-generating land use simulation (PLUS) model: A case study in Wuhan, China. *Comput. Environ. Urban Syst.* **2021**, *85*, 101569. [[CrossRef](#)]
29. Wu, H.; Luo, W.; Lin, A.; Hao, F.; Olteanu-Raimond, A.-M.; Liu, L.; Li, Y. SALT: A multifeature ensemble learning framework for mapping urban functional zones from VGI data and VHR images. *Comput. Environ. Urban Syst.* **2023**, *100*, 101921. [[CrossRef](#)]
30. Sankarrao, L.; Ghose, D.K.; Rathinsamy, M. Predicting land-use change: Intercomparison of different hybrid machine learning models. *Environ. Model. Softw.* **2021**, *145*, 105207. [[CrossRef](#)]
31. Lyu, R.; Mi, L.; Zhang, J.; Xu, M.; Li, J. Modeling the effects of urban expansion on regional carbon storage by coupling SLEUTH-3r model and InVEST model. *Ecol. Res.* **2019**, *34*, 380–393. [[CrossRef](#)]
32. Cao, M.; Zhu, Y.; Quan, J.; Zhou, S.; Lü, G.; Chen, M.; Huang, M. Spatial Sequential Modeling and Predication of Global Land Use and Land Cover Changes by Integrating a Global Change Assessment Model and Cellular Automata. *Earth's Future* **2019**, *7*, 1102–1116. [[CrossRef](#)]
33. Guan, Q.; Shi, X.; Huang, M.; Lai, C. A hybrid parallel cellular automata model for urban growth simulation over GPU/CPU heterogeneous architectures. *Int. J. Geogr. Inf. Sci.* **2016**, *30*, 494–514. [[CrossRef](#)]
34. Marques-Carvalho, R.; Almeida, C.M.d.; Escobar-Silva, E.V.; Oliveira Alves, R.B.d.; Anjos Lacerda, C.S.d. Simulation and Prediction of Urban Land Use Change Considering Multiple Classes and Transitions by Means of Random Change Allocation Algorithms. *Remote Sens.* **2023**, *15*, 90. [[CrossRef](#)]
35. Wang, J.; Zhang, J.; Xiong, N.; Liang, B.; Wang, Z.; Cressey, E.L. Spatial and Temporal Variation, Simulation and Prediction of Land Use in Ecological Conservation Area of Western Beijing. *Remote Sens.* **2022**, *14*, 1452. [[CrossRef](#)]
36. Liu, X.; Liang, X.; Li, X.; Xu, X.; Ou, J.; Chen, Y.; Li, S.; Wang, S.; Pei, F. A future land use simulation model (FLUS) for simulating multiple land use scenarios by coupling human and natural effects. *Landsc. Urban Plan.* **2017**, *168*, 94–116. [[CrossRef](#)]
37. Jin, T.; Zhang, X.; Wang, T.; Liang, J.; Ma, W.; Xie, J. Spatiotemporal impacts of climate change and human activities on blue and green water resources in northwest river basins of China. *Ecol. Indic.* **2024**, *160*, 111823. [[CrossRef](#)]
38. Wen, X.; Liu, D.; Qiu, M.; Wang, Y.; Niu, J.; Liu, Y. Estimation of maize yield incorporating the synergistic effect of climatic and land use change in Jilin, China. *J. Geogr. Sci.* **2023**, *33*, 1725–1746. [[CrossRef](#)]
39. Xiao, Y.; Huang, M.; Xie, G.; Zhen, L. Evaluating the impacts of land use change on ecosystem service values under multiple scenarios in the Hunshandake region of China. *Sci. Total Environ.* **2022**, *850*, 158067. [[CrossRef](#)]
40. Wu, S.; Wang, D.; Yan, Z.; Wang, X.; Han, J. Spatiotemporal dynamics of urban green space in Changchun: Changes, transformations, landscape patterns, and drivers. *Ecol. Indic.* **2023**, *147*, 109958. [[CrossRef](#)]
41. Xiong, S.; Yang, F.; Zhang, J.; Tang, Y. An integrated model chain for diagnosing and predicting conflicts between production-living-ecological space in lake network regions: A case of the Dongting Lake region, China. *Ecol. Indic.* **2024**, *166*, 112237. [[CrossRef](#)]
42. Chen, M.; Qian, Z.; Boers, N.; Jakeman, A.J.; Kettner, A.J.; Brandt, M.; Kwan, M.-P.; Batty, M.; Li, W.; Zhu, R.; et al. Iterative integration of deep learning in hybrid Earth surface system modelling. *Nat. Rev. Earth Environ.* **2023**, *4*, 568–581. [[CrossRef](#)]

43. Gomes, E.; Inácio, M.; Bogdzevič, K.; Kalinauskas, M.; Karnauskaitė, D.; Pereira, P. Future scenarios impact on land use change and habitat quality in Lithuania. *Environ. Res.* **2021**, *197*, 111101. [[CrossRef](#)] [[PubMed](#)]
44. Raji, S.A.; Odunuga, S.; Fasona, M. Spatially Explicit Scenario Analysis of Habitat Quality in a Tropical Semi-arid Zone: Case Study of the Sokoto–Rima Basin. *J. Geovisualization Spat. Anal.* **2022**, *6*, 11. [[CrossRef](#)]
45. Fida, G.T.; Baatuuwue, B.N.; Issifu, H. Potential impact of future land use/cover dynamics on the habitat quality of the Yayo Coffee Forest Biosphere Reserve, southwestern Ethiopia. *Geocarto Int.* **2024**, *39*, 2278327. [[CrossRef](#)]
46. Rahimi, L.; Malekmohammadi, B.; Yavari, A.R. Assessing and Modeling the Impacts of Wetland Land Cover Changes on Water Provision and Habitat Quality Ecosystem Services. *Nat. Resour. Res.* **2020**, *29*, 3701–3718. [[CrossRef](#)]
47. Kuang, W.; Du, G.; Lu, D.; Dou, Y.; Li, X.; Zhang, S.; Chi, W.; Dong, J.; Chen, G.; Yin, Z.; et al. Global observation of urban expansion and land-cover dynamics using satellite big-data. *Sci. Bull.* **2021**, *66*, 297–300. [[CrossRef](#)]
48. Li, F.; Li, Z.; Chen, H.; Chen, Z.; Li, M. An agent-based learning-embedded model (ABM-learning) for urban land use planning: A case study of residential land growth simulation in Shenzhen, China. *Land Use Policy* **2020**, *95*, 104620. [[CrossRef](#)]
49. Wang, Q.; Liu, D.; Gao, F.; Zheng, X.; Shang, Y. A Partitioned and Heterogeneous Land-Use Simulation Model by Integrating CA and Markov Model. *Land* **2023**, *12*, 409. [[CrossRef](#)]
50. Xu, Q.; Zhu, A.X.; Liu, J. Land-use change modeling with cellular automata using land natural evolution unit. *CATENA* **2023**, *224*, 106998. [[CrossRef](#)]
51. Li, S.; Zhuang, C.; Tan, Z.; Gao, F.; Lai, Z.; Wu, Z. Inferring the trip purposes and uncovering spatio-temporal activity patterns from dockless shared bike dataset in Shenzhen, China. *J. Transp. Geogr.* **2021**, *91*, 102974. [[CrossRef](#)]
52. Wang, S.; Song, Q.; Zhao, J.; Lu, Z.; Zhang, H. Identification of Key Areas and Early-Warning Points for Ecological Protection and Restoration in the Yellow River Source Area Based on Ecological Security Pattern. *Land* **2023**, *12*, 1643. [[CrossRef](#)]
53. Qi, J.; Wang, Z.; Cressey, E.L.; Liang, B.; Wang, J. Considering the Joint Impact of Carbon Density Change and Land Use Change Is Crucial to Improving Ecosystem Carbon Stock Assessment in North China. *Forests* **2024**, *15*, 55. [[CrossRef](#)]
54. Ding, Q.; Chen, Y.; Bu, L.; Ye, Y. Multi-Scenario Analysis of Habitat Quality in the Yellow River Delta by Coupling FLUS with InVEST Model. *Int. J. Environ. Res. Public Health* **2021**, *18*, 2389. [[CrossRef](#)]
55. Li, M.; Zhou, Y.; Xiao, P.; Tian, Y.; Huang, H.; Xiao, L. Evolution of Habitat Quality and Its Topographic Gradient Effect in Northwest Hubei Province from 2000 to 2020 Based on the InVEST Model. *Land* **2021**, *10*, 857. [[CrossRef](#)]
56. Wu, L.; Sun, C.; Fan, F. Estimating the Characteristic Spatiotemporal Variation in Habitat Quality Using the InVEST Model—A Case Study from Guangdong–Hong Kong–Macao Greater Bay Area. *Remote Sens.* **2021**, *13*, 1008. [[CrossRef](#)]
57. Chen, C.; Liu, J.; Bi, L. Spatial and Temporal Changes of Habitat Quality and Its Influential Factors in China Based on the InVEST Model. *Forests* **2023**, *14*, 374. [[CrossRef](#)]
58. Xiang, Q.; Kan, A.; Yu, X.; Liu, F.; Huang, H.; Li, W.; Gao, R. Assessment of Topographic Effect on Habitat Quality in Mountainous Area Using InVEST Model. *Land* **2023**, *12*, 186. [[CrossRef](#)]
59. Wang, B.; Cheng, W. Effects of Land Use/Cover on Regional Habitat Quality under Different Geomorphic Types Based on InVEST Model. *Remote Sens.* **2022**, *14*, 1279. [[CrossRef](#)]
60. Wang, B.; Oguchi, T.; Liang, X. Evaluating future habitat quality responding to land use change under different city compaction scenarios in Southern China. *Cities* **2023**, *140*, 104410. [[CrossRef](#)]
61. Zeng, W.; Tang, H.; Liang, X.; Hu, Z.; Yang, Z.; Guan, Q. Using ecological security pattern to identify priority protected areas: A case study in the Wuhan Metropolitan Area, China. *Ecol. Indic.* **2023**, *148*, 110121. [[CrossRef](#)]
62. Berta Aneseyee, A.; Noszczyk, T.; Soromessa, T.; Elias, E. The InVEST Habitat Quality Model Associated with Land Use/Cover Changes: A Qualitative Case Study of the Winike Watershed in the Omo-Gibe Basin, Southwest Ethiopia. *Remote Sens.* **2020**, *12*, 1103. [[CrossRef](#)]
63. Guan, X.; Li, J.; Yang, C.; Xing, W. Development Process, Quantitative Models, and Future Directions in Driving Analysis of Urban Expansion. *ISPRS Int. J. Geo-Inf.* **2023**, *12*, 174. [[CrossRef](#)]
64. He, J.; Li, C.; Yu, Y.; Liu, Y.; Huang, J. Measuring urban spatial interaction in Wuhan Urban Agglomeration, Central China: A spatially explicit approach. *Sustain. Cities Soc.* **2017**, *32*, 569–583. [[CrossRef](#)]
65. Lin, J.; Li, X.; Wen, Y.; He, P. Modeling urban land-use changes using a landscape-driven patch-based cellular automaton (LP-CA). *Cities* **2023**, *132*, 103906. [[CrossRef](#)]
66. Zhang, C.; Wang, P.; Xiong, P.; Li, C.; Quan, B. Spatial Pattern Simulation of Land Use Based on FLUS Model under Ecological Protection: A Case Study of Hengyang City. *Sustainability* **2021**, *13*, 10458. [[CrossRef](#)]
67. Huang, J.; Lu, X.; Wang, Y. Spatio–Temporal Changes and Key Driving Factors of Urban Green Space Configuration on Land Surface Temperature. *Forests* **2024**, *15*, 812. [[CrossRef](#)]
68. Wang, H.; Lin, C.; Ou, S.; Feng, Q.; Guo, K.; Xie, J.; Wei, X. Evolutionary Characteristics and Driving Forces of Green Space in Guangzhou from a Zoning Perspective. *Forests* **2024**, *15*, 135. [[CrossRef](#)]
69. Wu, J.; Li, X.; Luo, Y.; Zhang, D. Spatiotemporal effects of urban sprawl on habitat quality in the Pearl River Delta from 1990 to 2018. *Sci. Rep.* **2021**, *11*, 13981. [[CrossRef](#)]

70. Liu, J.; Li, S.; Ouyang, Z.; Tam, C.; Chen, X. Ecological and socioeconomic effects of China's policies for ecosystem services. *Proc. Natl. Acad. Sci. USA* **2008**, *105*, 9477–9482. [[CrossRef](#)]
71. Zhong, J.; Jiao, L.; Droin, A.; Liu, J.; Lian, X.; Taubenböck, H. Greener cities cost more green: Examining the impacts of different urban expansion patterns on NPP. *Build. Environ.* **2023**, *228*, 109876. [[CrossRef](#)]
72. Shu, B.; Zhu, S.; Qu, Y.; Zhang, H.; Li, X.; Carsjens, G.J. Modelling multi-regional urban growth with multilevel logistic cellular automata. *Comput. Environ. Urban Syst.* **2020**, *80*, 101457. [[CrossRef](#)]
73. Zeng, C.; Stringer, L.C.; Lv, T. The spatial spillover effect of fossil fuel energy trade on CO<sub>2</sub> emissions. *Energy* **2021**, *223*, 120038. [[CrossRef](#)]
74. Wu, X.; Pan, J.; Zhu, X. Optimizing the ecological source area identification method and building ecological corridor using a genetic algorithm: A case study in Weihe River Basin, NW China. *Ecol. Inform.* **2024**, *80*, 102519. [[CrossRef](#)]
75. Huang, Y.; Lin, J.; He, X.; Lin, Z.; Wu, Z.; Zhang, X. Assessing the scale effect of urban vertical patterns on urban waterlogging: An empirical study in Shenzhen. *Environ. Impact Assess. Rev.* **2024**, *106*, 107486. [[CrossRef](#)]
76. Yuan, R.; Zhang, N.; Zhang, Q. The impact of habitat loss and fragmentation on biodiversity in global protected areas. *Sci. Total Environ.* **2024**, *931*, 173004. [[CrossRef](#)]
77. Barlow, J.; Lennox, G.D.; Ferreira, J.; Berenguer, E.; Lees, A.C.; Nally, R.M.; Thomson, J.R.; Ferraz, S.F.d.B.; Louzada, J.; Oliveira, V.H.F.; et al. Anthropogenic disturbance in tropical forests can double biodiversity loss from deforestation. *Nature* **2016**, *535*, 144–147. [[CrossRef](#)]
78. Zhu, W.; Jin, X.; Zhang, X.; Liu, J.; Zhou, Y. Ecosystem services to support sustainable development: The modifiable areal unit problem in the transition between evaluation and management units. *Sustain. Dev.* **2024**, *32*, 6253–6273. [[CrossRef](#)]
79. Li, Y.; Hu, B.; Zhang, D.; Gong, J.; Song, Y.; Sun, J. Flood evacuation simulations using cellular automata and multiagent systems—a human-environment relationship perspective. *Int. J. Geogr. Inf. Sci.* **2019**, *33*, 2241–2258. [[CrossRef](#)]
80. Yu, H.; Tu, Z.; Yu, G.; Xu, L.; Wang, H.; Yang, Y. Shrinkage and protection of inland lakes on the regional scale: A case study of Hubei Province, China. *Reg. Environ. Change* **2020**, *20*, 4. [[CrossRef](#)]
81. Liu, Z.; Verburg, P.H.; Wu, J.; He, C. Understanding Land System Change Through Scenario-Based Simulations: A Case Study from the Drylands in Northern China. *Environ. Manag.* **2017**, *59*, 440–454. [[CrossRef](#)] [[PubMed](#)]
82. Mozaffaree Pour, N.; Karasov, O.; Burdun, I.; Oja, T. Simulation of land use/land cover changes and urban expansion in Estonia by a hybrid ANN-CA-MCA model and utilizing spectral-textural indices. *Environ. Monit. Assess.* **2022**, *194*, 584. [[CrossRef](#)] [[PubMed](#)]
83. Yin, H.; Kong, F.; Dronova, I. Hydrological performance of extensive green roofs in response to different rain events in a subtropical monsoon climate. *Landsc. Ecol. Eng.* **2019**, *15*, 297–313. [[CrossRef](#)]
84. Lu, S.; Xiao, Y.; Lu, Y.; Lin, J. Spatialization of electricity consumption by combining high-resolution nighttime light remote sensing and urban functional zoning information. *Geo-Spat. Inf. Sci.* **2024**. [[CrossRef](#)]
85. Yue, W.; Feng, B.; Zhou, Q.; Xu, R.; Li, M. An assessment of the Ecological Conservation Redline: Unlocking priority areas for conservation. *J. Environ. Plan. Manag.* **2024**, *67*, 1034–1052. [[CrossRef](#)]
86. Fan, Z. Simulation of land-cover change in Jing-Jin-Ji region under different scenarios of SSP-RCP. *J. Geogr. Sci.* **2022**, *32*, 421–440. [[CrossRef](#)]
87. Zaki, A.; Buchori, I.; Pangli, P.; Sejati, A.W.; Liu, Y. Google Earth Engine for improved spatial planning in agricultural and forested lands: A method for projecting future ecological quality. *Remote Sens. Appl. Soc. Environ.* **2023**, *32*, 101078. [[CrossRef](#)]
88. Abolhasani, S.; Taleai, M.; Lakes, T. Developing a game-theoretic interactive decision-making framework for urban land-use planning. *Habitat Int.* **2023**, *141*, 102930. [[CrossRef](#)]
89. Yao, Y.; Zhang, H.; Sun, Z.; Li, L.; Cheng, T.; Jiang, Y.; Guan, Q.; Chen, D. Fine-grained regional economic forecasting for a megacity using vector-based cellular automata. *Int. J. Appl. Earth Obs. Geoinf.* **2023**, *125*, 103602. [[CrossRef](#)]
90. Zhao, X.; Ma, X.; Tang, W.; Liu, D. An adaptive agent-based optimization model for spatial planning: A case study of Anyue County, China. *Sustain. Cities Soc.* **2019**, *51*, 101733. [[CrossRef](#)]
91. Yang, L.; Li, X.; Yang, Q.; Zhang, L.; Zhang, S.; Wu, S.; Zhou, C. Extracting knowledge from legacy maps to delineate eco-geographical regions. *Int. J. Geogr. Inf. Sci.* **2021**, *35*, 250–272. [[CrossRef](#)]
92. van Duynhoven, A.; Dragičević, S. A landscape metrics-based sample weighting approach for forecasting land cover change with deep learning models. *Geocarto Int.* **2023**, *38*, 2240283. [[CrossRef](#)]
93. Hanoon, S.K.; Abdullah, A.F.; Shafri, H.Z.M.; Wayayok, A. Urban Growth Forecast Using Machine Learning Algorithms and GIS-Based Novel Techniques: A Case Study Focusing on Nasiriyah City, Southern Iraq. *ISPRS Int. J. Geo-Inf.* **2023**, *12*, 76. [[CrossRef](#)]
94. Yu, Y.; He, J.; Tang, W.; Li, C. Modeling Urban Collaborative Growth Dynamics Using a Multiscale Simulation Model for the Wuhan Urban Agglomeration Area, China. *ISPRS Int. J. Geo-Inf.* **2018**, *7*, 176. [[CrossRef](#)]
95. Yang, J.; Yang, Y.; Sun, D.; Jin, C.; Xiao, X. Influence of urban morphological characteristics on thermal environment. *Sustain. Cities Soc.* **2021**, *72*, 103045. [[CrossRef](#)]

96. Chambers-Ostler, A.; Walker, H.; Doick, K.J. The role of the private tree in bringing diversity and resilience to the urban forest. *Urban For. Urban Green.* **2024**, *91*, 127973. [[CrossRef](#)]
97. Xu, S.; Zou, B.; Shafi, S.; Sternberg, T. A hybrid Grey-Markov/ LUR model for PM10 concentration prediction under future urban scenarios. *Atmos. Environ.* **2018**, *187*, 401–409. [[CrossRef](#)]
98. Kirschner, V.; Macků, K.; Moravec, D.; Mañas, J. Measuring the relationships between various urban green spaces and local climate zones. *Sci. Rep.* **2023**, *13*, 9799. [[CrossRef](#)]
99. Guo, X.; Zhang, H.; Wu, Z.; Zhao, J.; Zhang, Z. Comparison and Evaluation of Annual NDVI Time Series in China Derived from the NOAA AVHRR LTDR and Terra MODIS MOD13C1 Products. *Sensors* **2017**, *17*, 1298. [[CrossRef](#)]
100. Li, X.; Xu, H.; Ma, X.; Huang, Y. A two-step spatially explicit optimization approach of integrating ecosystem services (ES) into land use planning (LUP) to generate the optimally sustainable schemes. *Land Degrad. Dev.* **2023**, *34*, 2508–2522. [[CrossRef](#)]
101. Zhang, X.; Jin, X.; Liang, X.; Ren, J.; Han, B.; Liu, J.; Fan, Y.; Zhou, Y. Implications of land sparing and sharing for maintaining regional ecosystem services: An empirical study from a suitable area for agricultural production in China. *Sci. Total Environ.* **2022**, *820*, 153330. [[CrossRef](#)] [[PubMed](#)]
102. Ma, X.; Peng, S. Research on the spatiotemporal coupling relationships between land use/land cover compositions or patterns and the surface urban heat island effect. *Environ. Sci. Pollut. Res.* **2022**, *29*, 39723–39742. [[CrossRef](#)] [[PubMed](#)]
103. Woodman, T.L.; Rueda-Urbe, C.; Henry, R.C.; Burslem, D.F.R.P.; Travis, J.M.J.; Alexander, P. Introducing LandScaleR: A novel method for spatial downscaling of land use projections. *Environ. Model. Softw.* **2023**, *169*, 105826. [[CrossRef](#)]
104. Wang, H.; Zhang, B.; Xia, C.; He, S.; Zhang, W. Using a maximum entropy model to optimize the stochastic component of urban cellular automata models. *Int. J. Geogr. Inf. Sci.* **2020**, *34*, 924–946. [[CrossRef](#)]
105. Jiang, L.; Liu, Y. Dynamic assessment of the COVID-19 lockdown in the Xinjiang region using night-time light remote sensing. *Int. J. Digit. Earth* **2024**, *17*, 2300317. [[CrossRef](#)]
106. Viana, C.M.; Pontius, R.G., Jr.; Rocha, J. Four Fundamental Questions to Evaluate Land Change Models with an Illustration of a Cellular Automata–Markov Model. *Ann. Am. Assoc. Geogr.* **2023**, *113*, 2497–2511. [[CrossRef](#)]
107. Long, Y.; Wu, K. Simulating Block-Level Urban Expansion for National Wide Cities. *Sustainability* **2017**, *9*, 879. [[CrossRef](#)]
108. Yang, J.; Sun, Y.; Zhu, J.; Song, S. Simulating urban land-use change based on the multi-hierarchical planning–environment interaction process. *Trans. GIS* **2023**, *27*, 152–175. [[CrossRef](#)]
109. Cui, L.; Berger, U.; Cao, M.; Zhang, Y.; He, J.; Pan, L.; Jiang, J. Conservation and Restoration of Mangroves in Response to Invasion of *Spartina alterniflora* Based on the MaxEnt Model: A Case Study in China. *Forests* **2023**, *14*, 1220. [[CrossRef](#)]
110. Deng, Z.; Quan, B.; Zhang, H.; Xie, H.; Zhou, Z. Scenario Simulation of Land Use and Cover under Safeguarding Ecological Security: A Case Study of Chang-Zhu-Tan Metropolitan Area, China. *Forests* **2023**, *14*, 2131. [[CrossRef](#)]
111. Ren, H.; Zhang, J.; Zhu, W.; Wang, L.; Zhang, L.; Zhu, L. Impact of land use change on habitat in the Qihe River Basin of Taihang Mountains. *Prog. Geogr.* **2018**, *37*, 1693–1704. [[CrossRef](#)]
112. Hack, J.; Molewijk, D.; Beißler, M.R. A Conceptual Approach to Modeling the Geospatial Impact of Typical Urban Threats on the Habitat Quality of River Corridors. *Remote Sens.* **2020**, *12*, 1345. [[CrossRef](#)]
113. Sallustio, L.; De Toni, A.; Strollo, A.; Di Febbraro, M.; Gissi, E.; Casella, L.; Geneletti, D.; Munafò, M.; Vizzarri, M.; Marchetti, M. Assessing habitat quality in relation to the spatial distribution of protected areas in Italy. *J. Environ. Manag.* **2017**, *201*, 129–137. [[CrossRef](#)] [[PubMed](#)]

**Disclaimer/Publisher’s Note:** The statements, opinions and data contained in all publications are solely those of the individual author(s) and contributor(s) and not of MDPI and/or the editor(s). MDPI and/or the editor(s) disclaim responsibility for any injury to people or property resulting from any ideas, methods, instructions or products referred to in the content.